ORIGINAL PAPER

Dynamic motion of La atom inside the C_{74} (D_{3h}) cage: a relativistic DFT study

Dongxu Tian · Suzhen Ren · Ce Hao

Abstract The interaction between lanthanum atom (La) and C_{74} (D_{3h}) was investigated by all-electron relativistic density function theory (DFT). With the aid of the representative patch of C_{74} (D_{3h}), we studied the interaction between C_{74} (D_{3h}) and La and obtained the interaction potential. Optimized structures show that there are three equivalent stable isomers, with La located about 1.7 Å off center. There is one transition state between every two stable isomers. According to the minimum energy pathway, the possible movement trajectory of La atoms in the C_{74} (D_{3h}) cage was explored. The calculated energy barrier for La atoms moving from the stable isomer to the transition state is 18.4 kcal mol^{-1}. In addition, the dynamic NMR spectra of La@C_{74} according to the trajectory was calculated.

Keywords Relativistic DFT · La@C_{74} · Energy potential surface · Dynamic NMR

Introduction

Since the first extraction of metallofullerene La@C_{82} [1], endohedral metallofullerenes (EMFs) have attracted considerable attention [2, 3] due to their novel structures with promising properties and applications in material and biological science. C_{74} is very unstable and is called a "missing fullerene" among the fullerene family. However, the C_{74} cage is stabilized when a divalent metal (M) is inserted into the cage, with two electrons transferred from the metal to the C_{74} cage [4]. Experimentally, some divalent M^{2+}@C_{74}^{2-} EMFs(M = Ba [5–7], Eu [8], Sm [9–11], Ca [6, 12], Sr [6, 7], or Yb [13]) have been isolated. M^{2+}@C_{74}^{2-} has been characterized by UV–VIS, Raman, and EPR spectroscopy.

D. Tian · S. Ren · C. Hao (✉)
State Key Laboratory of Fine Chemicals, Dalian University of Technology, Dalian 116024, People's Republic of China
e-mail: haoce@dlut.edu.cn

However, insoluble EMFs, such as La@C_{74}, have not yet been isolated, although they are observed regularly in raw soot by mass spectrometry. Nikawa et al. [3] first reported isolation of La@C_{74} as an EMF derivative, La@C_{74} ($C_6H_3Cl_2$), suggesting that La@C_{74} has an electronic structure of La^{3+}@C_{74}^{3-} and is paramagnetic.

The position and motion of the encapsulated metal atom plays an important role in the chemical and physical properties of EMFs. Both experimental and theoretical studies have revealed the dynamic behavior of metal atoms encapsulated in pristine and functionalized fullerene cages. Experimentally, Miyake et al. [14] have studied the motion of the scandium ions in Sc$_2$@C_{84} by ^{45}Sc solution NMR spectroscopy. The two scandium ions in Sc$_2$@C_{84} with D_{2d} symmetry rapidly change their positions. Nishibori et al. [15] reported that the trajectory of lanthanum atoms is like a bowl or hemisphere in C_{82} cages at room temperature using the maximum entropy method (MEM). Recently, ^{13}C NMR spectroscopy strongly suggests that two encapsulated Lu atoms rapidly rotate in T_d-C_{76} fullerene cages [16]. A similar dynamical motion of encaged metal atoms in fullerenes has been observed in La$_2$@C_{80} [17, 18]. Theoretically, Andreoni et al. [19] obtained the dynamic trajectory of La inside C_{60} by ab initio molecular dynamics. Heine et al. calculated the dynamic NMR spectra [20] of Sc$_3$N@C_{80} using quantum Born-Oppenheimer molecular dynamics simulations, followed by DFT-NMR calculations on a large series of snapshots. Jin et al. [21] reported that the La atom probably undergoes boat-shaped movement at high temperatures. Moreover, dynamical motion of divalent metals in C_{74} (D_{3h}) cages has been investigated. The ^{13}C NMR spectra of Ca@C_{74} indicate that the Ca atom hops inside the D_{3h} cage [22]. A similar dynamic motion has been observed in Yb@C_{74} by ^{13}C NMR spectroscopy [4]. The dynamic behavior of europium in Eu@C_{74} was investigated by quasi-relativistic density-functional based tight binding calculations and molecular dynamics simulations by Viezte et al. [23]. To the best of our knowledge, few

theoretical studies have been reported with the purpose of exploring the dynamic behavior of lanthanum atoms in C_{74} (D_{3h}) cages. $La^{3+}@C_{74}^{3-}$ is different from divalent $M^{2+}@C_{74}^{2-}$ EMFs because of the different electronic structure. Two questions are important in the study of the La@C_{74} system. Does the trivalent La ion show dynamic motion in the C_{74} (D_{3h}) cage? And, what is the trajectory of the La ion in C_{74} (D_{3h}) cage?

In this study, the interaction between the La atom and the C_{74} (D_{3h}) cage is analyzed using all-electron relativistic DFT considering the representative patch of C_{74} (D_{3h}). We optimized all possible isomers, searched for all transition states, and calculated the activation energies and the linear synchronous transit (LST). With the aid of the potential energy surface (PES) obtained by a single point energy scan over the σ_h surface of the cage, the motion of La in the cage is clarified. Furthermore, the trajectory of the La atom in the C_{74} (D_{3h}) cage and the dynamic NMR spectra of La@C_{74} were obtained.

Computational details

The DFT calculations of La@C_{74} were performed using the Dmol3 code [24, 25], and the Becke-Lee-Yang-Parr (BLYP) exchange correlation functional, which is a combination of the Becke exchange functional [26] coupled with the Lee-Yang-Parr (LYP) correlation potential [27]. The basis sets used in this work were double-numerical quality basis sets with polarization functions (DNP), which is comparable to the Gaussian 6–31 G** basis set. It is known that relativistic effects play an important role in the chemical and physical properties of molecules containing heavy elements such as Lanthanide [28–33]. To take into account relativistic effects, the all-electron scalar relativistic method using the Douglas-Kroll-Hess (DKH) Hamiltonian, the most accurate approach available in Dmol3, was chosen. Self-consistent field procedures were carried out with a

convergence criterion of 10^{-6} a.u. on the energy and electron density. Full geometry optimizations were performed using the Broyden-Fletcher-Goldfarb-Shanno (BFGS) algorithm [34] with a convergence criterion of 10^{-3} a.u. on the displacement and 10^{-5} a.u. on the energy. The transition states were searched using the complete LST/QST method with a convergence criterion of 0.002 a.u. on the RMS [35].

The NMR spectra of $[La@C_{74}]^{-}$ was calculated using the ADF2008.01 program [36, 37], with the BLYP exchange correlation functional and the TZP basis set. The configurations were calculated by using the zero-order regular approximation (ZORA) [38–40], in which relativistic effects are considered.

Results and discussion

Geometry optimization and transition state search

The hollow C_{74} cage with D_{3h} symmetry was optimized, and then full geometry optimizations were carried out for La@C_{74} to find the favorable position for the La, with the most stable structure of La@C_{74} shown in Fig. 1a. The point group symmetry of La@C_{74} becomes C_{2v} upon encapsulation of the La atom. The La atom is located about 1.7 Å off-center and under a [6] double bond along a C_2 axis on the σ_h plane. The vibrational frequencies of La@C_{74} were computed and all turned out to be real, ensuring that the configuration was a true minimum. Three symmetrically equivalent stable sites for the La atom were found inside the cage along the three C_2 axes on the σ_h plane due to the D_{3h} symmetry of the cage.

Because there are three equivalent sites for the La atom, which are linked by rotation around the threefold axis, there is a transition state (TS) between two such equivalent minima. The TS structure (Fig. 1b) shows that La is located about 1.5 Å off-center along the C_2 axis, and is under a hexagon opposite to the C=C double bond on the σ_h plane.

Fig. 1 **a** Structure of La@C_{74} optimized by all-electron relativistic density functional theory Becke-Lee-Yang-Parr with double-numerical quality basis sets with polarization functions (DFT BLYP/DNP). **b** Optimized transition state
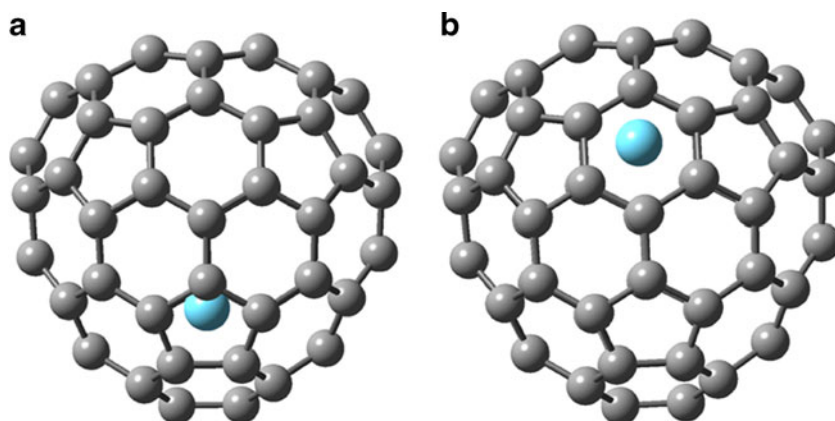
Table 1 Calculated geometric and energetic parameters of La@C$_{74}$. *TS* Transition state

La@C$_{74}$	R_{La-C}(Å)[a]	E (kcal mol^{-1})[b]	E (kcal mol^{-1})[c]	AE (kcal mol^{-1})[d]
Energy stationary point	2.518	0	278.1	0
TS	2.585	19.3	277.1	18.4

[a] Shortest La-C distance

[b] Relative total energy

[c] Zero-point vibration energy

[d] Activation energy

The structure of the transition state also has C_{2v} symmetry. The TS is a saddle point, since it has an imaginary frequency of 63.5 i cm^{-1}.

Table 1 shows the shortest La–C distances and the energy parameters of the two configurations. The lowest energy of the most stable configuration was taken as the relative zero point energy. The activation energy between the minimum energy point and the saddle point is 18.4 kcal mol^{-1}.

Interaction between La and C$_{74}$ (D$_{3h}$)

Representative patch for C$_{74}$ (D$_{3h}$)

C$_{74}$ fullerene has only one isomer that satisfies the isolated pentagon rule with D_{3h} symmetry. A right angle patch under a circum-spherical surface was taken as a representative patch of the C$_{74}$ (D$_{3h}$) cage to describe the symmetry of a C$_{74}$ (D$_{3h}$) cage simply as shown in Fig. 2.

The area of the patch LMN is equal to 1/12 of the total surface area. There are 27 key points on the C$_{74}$(D$_{3h}$) representative patch. Points C1–C9 represent nine different
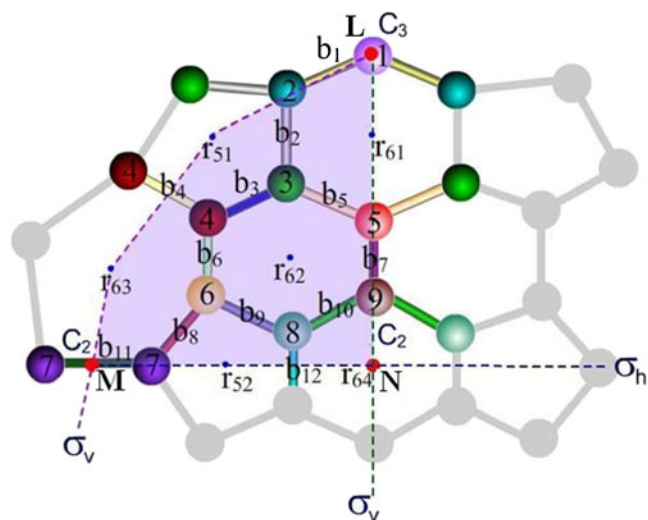
types of carbon atoms: C1 has C_{3v} local symmetry; C2, C5, C7, C9 have C_s local symmetry; and C3, C4, C6, C8 have C_1 local symmetry. Points b_1 to b_{12} represent the 12 distinct C—C bonds: b_{11} has C_{2v} local symmetry; and b_n (n=2, 3, 5, 6, 8, 9, and 10) have C_1 local symmetry. r_{61} to r_{64} denote the four types of six-membered rings: r_{61} and r_{63} have C_s local symmetry; r_{64} has C_{2v} local symmetry. r_{51} and r_{52} represent the two types of five-membered rings with C_s local symmetry. When 12 elements of the D_{3h} group are operated on the patch, the patch will encompass the entire surface of the polyhedron.

Interaction between La and C$_{74}$ (D$_{3h}$)

The interaction energy of La–C$_{74}$(D_{3h}) was calculated. Firstly, the C$_{74}$(D_{3h}) cage was fixed, and then the La atom was allowed to approach the 27 key points along the radial directions, which pass through the center of the cage and the key points. The calculated potential energy curves as a function of the distance between the La atom and the key points are shown in Fig. 3. There is a minimum energy point in each potential energy curve. These energy minima are located between 1.6 and 1.8 Å from the center of the cage. The five minimum energy lines are C7, b_{11}, r_{52}, b_{12} and r_{64}, all of which are located in the σ_h plane. To clarify the minimum energy pathway, the σ_h plane should be studied in detail.

The PES of the σ_h plane was obtained using the single point energy scan as shown in Fig. 4a. There are three equivalent local minima on the σ_h surface, denoted by A, that are about 1.7 Å off-center. The transition states B are about 1.5 Å off-center. As shown in Fig. 4a, the relative energy between A and B is about 18.4 kcal mol^{-1}, which is consistent with the value from the geometry optimization listed in Table 1. The lowest energy pathway is in the σ_h

Fig. 2 Representative patch of the C$_{74}$ (D$_{3h}$) cage (*shaded*)
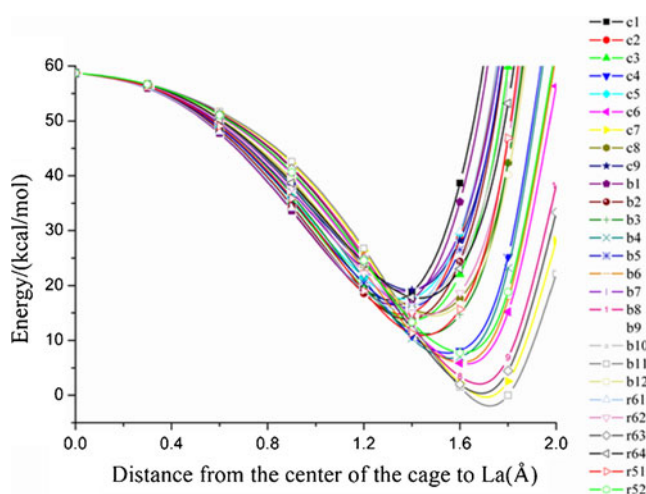
Fig. 3 Calculated potential energy curves of La atoms approaching the 27 key points of the C$_{74}$ cage (BLYP/DNP)

Fig. 4 **a** Calculated potential energy surface (PES) of La atom on the σh surface of the C74 (D3h) cage at BLYP/DNP level (energy in eV). **b** Probable trajectory of the La atom in the cage
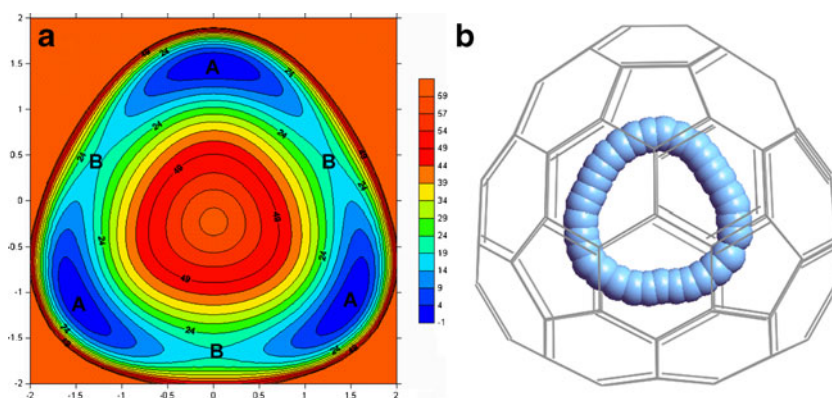
plane(A-B-A-B-A-B-A). It is proposed that the motion of La forms a ring. The motion of La in the C_{74} (D_{3h}) cage forms a ring as shown in Fig. 4b. The trajectory of La has D_{3h} symmetry and is in the σ_h plane. It is reasonable to predict the motion of the atom inside the cage by comparing the energy of different configurations.

Prediction of ^{13}C NMR spectrum

Using the trajectory of La in the C_{74} (D_{3h}) cage, the ^{13}C NMR spectrum of La@C_{74} can be predicted. First, we qualitatively analyze the ^{13}C NMR spectrum of La@C_{74}. There should be nine lines that correspond to the nine types of atoms in the C_{74} (D_{3h}) cage. The nine carbon atoms are defined as shown in Fig. 2. We can predict the intensity of lines: C1 has C_{3v} local symmetry, so it should give 1/6 intensity signals; C2, C5, C7, C9 have C_s local symmetry, so should give half intensity signals; C3, C4, C6, C8 have C_1 local symmetry, so should give full intensity signals.

In addition, we calculated the average chemical shifts for all of the carbon atoms to simulate the dynamic ^{13}C NMR
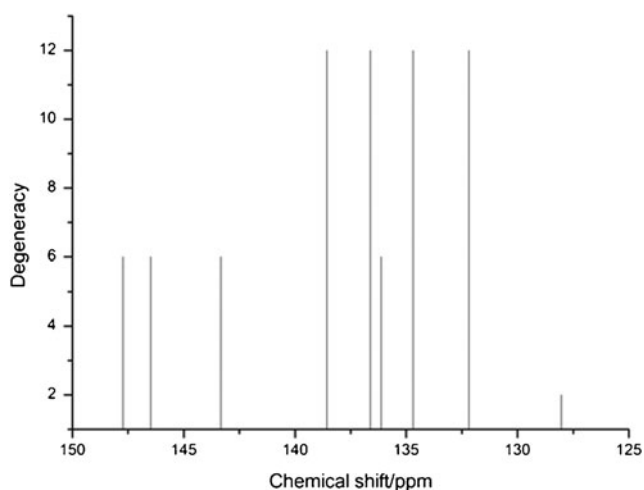
spectrum of La@C_{74}. The 74 C atoms were divided into nine groups according to the representative patch of C_{74} (D_{3h}), and their arithmetic average chemical shifts were obtained. Figure 5 shows the ^{13}C NMR spectrum of [La@C_{74}]⁻, with the calculated chemical shifts ranging from 128 to 147.7 ppm. The calculated chemical shieldings [δ(Ci)] were then referenced to those of C_{60} to obtain the calculated NMR chemical shifts using the following formula [41]:

$$\delta(Ci) = \delta(C_{60}) + \sigma(C_{60}) - \sigma(Ci), \tag{1}$$

where $\delta(C_{60})$ is taken to be 143.15 ppm [42], $\sigma(C_{60})$ is the calculated chemical shielding of C_{60} (28.30 ppm), and (Ci) is the carbon atom under consideration.

From Fig. 5, the ^{13}C NMR spectrum of [La@C_{74}]⁻ contains nine signals. The spectrum has four lines with full intensity, four lines with half intensity, and one line with 1/6 intensity. This means that there are nine types of carbon atoms in the metallofullerene cage. This NMR pattern indicates that La@C_{74} retains the D_{3h} symmetry of the C_{74} cage. These spectral features are similar to those of Ca@C_{74} [22] and Yb@C_{74} [4].

Computed [43] and experimental electronic, infrared and Raman spectra indicates that Eu@C_{74} has a C_{2v} symmetric structure derived from the D_{3h} symmetric IPR isomer of C_{74}. The results of a study by Rappoport and Furche [43] together with those of the present study demonstrate that computational works can help to interpret spectroscopic data and to assign structures.

Conclusions

In summary, we have investigated La@C_{74} by all-electron relativistic DFT. We obtained the lowest energy structure of La@C_{74} and the TS. Both configurations of the lowest energy structure and the TS have C_{2v} symmetry. The energy barrier is 18.4 kcal mol⁻¹ for La to hop from one stable site to another. The lowest energy pathway is in the σ_h plane,

Fig. 5 Calculated ^{13}C NMR spectrum of [La@C_{74}]⁻

and the trajectory is a ring with D_{3h} symmetry. On the basis of this, the dynamic ^{13}C NMR spectrum of La@C_{74} was predicted. There are 9 lines in the spectrum: four of them have full intensity, four have half intensity, and one has one-sixth intensity. This NMR pattern indicates that the system has D_{3h} symmetry, which is the same as the surrounding cage. This indicates the dynamic motion of the encaged metal atom and can be used to determine the dynamic motion of one or more atoms inside carbon cages.

References

1. Heath JR, O'Brien SC, Zhang Q, Liu Y, Curl RF (1985) Lanthanum complexes of spheroidal carbon shells. J Am Chem Soc 107:7779–7780
2. Chai Y, Guo T, Jin C, Haufler RE, Chibante LPF (1991) Fullerenes with metals inside. J Phys Chem 95:7564–7568
3. Nikawa H, Kikuchi T, Wakahara T, Nakahodo T, Tsuchiya T (2005) Missing metallofullerene La@C_{74}. J Am Chem Soc 127:9684–9685
4. Xu J, Tsuchiya T, Hao C, Shi Z, Wakahara T (2006) Structure determination of a missing-caged metallofullerene Yb@C_{74} (II) and the dynamic motion of the encaged ytterbium ion. Chem Phys Lett 419:44–47
5. Haufe O, Reich A, Möschel C, Jansen M (2001) Darstellung, Isolierung und Charakterisierung von Ba@C74.Z. Anorg Allg Chem 627:23–27
6. Grupp A, Haufe M, Jansen M, Mehring M, Panthofer J (2002) Synthesis, isolation and characterisation of New alkaline earth endohedral fullerenes M@C_n (M = Ca, Sr; n=74, 76). AIP Conference Proceedings 633:31–34
7. Haufe O, Hecht M, Grupp A, Mehring M, Jansen M (2005) Isolation and spectroscopic characterization of New endohedral fullerenes in the size gap of C_{74} to C_{76}. Z Anorg Allg Chem 631:126–130
8. Kuran P, Krause M, Bartl A, Dunsch L (1998) Preparation, isolation and characterisation of Eu@C74: the first isolated europium endohedral fullerene. Chem Phys Lett 292:580–586
9. Okazaki T, Lian Y, Gu ZN, Suenagac K, Shinohara H (2000) Isolation and spectroscopic characterization of Sm-containing metallofullerenes. Chem Phys Lett 320:435–440
10. Okazaki T, Suenaga K, Lian Y, Gu Z, Shinohara H (2001) Intrafullerene electron transfers in Sm-containing metallofullerenes Sm@C_{2n} (74≤2n≤84). J Mol Graph Model 19:244–251
11. Okazaki T, Suenaga K, Lian YF, Gu ZN, Shinohara H (2000) Direct EELS observation of the oxidation states of Sm atoms in Sm@C_{2n} metallofullerenes (74 ≤2n ≤84). J Chem Phys 113:9593–9597
12. Wan TSM, Zhang HW (1998) Production, isolation and electronic properties of missing fullerenes:Ca@C_{72} and Ca@C_{74}. J Am Chem Soc 120:6806–6807
13. Xu JX, Lu X, Zhou XH, He XR, Shi ZJ (2004) Synthesis, isolation and spectroscopic characterization of ytterbium-containing metallofullerenes. Chem Mater 16:2959–2964
14. Miyake Y, Suzuki S, Kojima Y, Kikuchi K, Kobayashi K (1996) Motion of scandium ions in Sc2C84 observed by ^{45}Sc solution NMR. J Phys Chem 100:9579–9581
15. Nishibori E, Takata M, Sakata M, Tanaka H, Hasegawa M (2000) Giant motion of La atom inside C_{82} cage. Chem Phys Lett 330:497–502
16. Umemoto H, Ohashi K, Inoue T, Fukui N, Sugai T (2010) Synthesis and UHV-STM observation of the T_d-symmetric Lu metallofullerene: Lu2@C_{76}(T_d). Chem Commun 46:5653–5655
17. Akasaka T, Nagase S, Kobayashi K, Wälchli M, Yamamoto K (1997) ^{13}C and ^{139}La NMR studies of La2@C_{80}: first evidence for circular motion of metal atoms in endohedral dimetallofullerenes. Angew Chem Int Ed Engl 36:1643–1645
18. Nishibori E, Takata M, Sakata M, Taninaka A, Shinohara H (2001) Pentagonal-dodecahedral La2 charge density in [80-I_h] fullerene: La2@C_{80}. Angew Chem Int Ed 40:2998–2999
19. Andreoni W, Curioni A (1996) Freedom and constraints of a metal atom encapsulated in fullerene cages. Phys Rev Lett 77:834–837
20. Heine T, Vietze K, Seifert G (2004) ^{13}C NMR fingerprint characterizes long time-scale structure of Sc3N@C_{80} endohedral fullerene. Magn Reson Chem 42:S199–S201
21. Jin P, Hao C, Li SM, Mi WH, Sun ZC (2006) Theoretical study on the motion of a La atom inside a C_{82} cage. J Phys Chem A 111:167–169
22. Kodama T, Fujii R, Miyake Y, Suzuki S, Nishikawa H (2004) 13C NMR study of Ca@C74: the cage structure and the site-hopping motion of a Ca atom inside the cage. Chem Phys Lett 399:94–97
23. Vietze K, Seifert G, Fowler PW (2000) Structure and dynamics of endohedral fullerenes. AIP Conf Proc 544:131–134
24. Delley B (1990) An all–electron numerical method for solving the local density functional for polyatomic molecules. J Chem Phys 92:508–517
25. Delley B (2000) From molecules to solids with the DMol^3 approach. J Chem Phys 113:7756–7764
26. Becke AD (1998) Density-functional exchange-energy approximation with correct asymptotic behavior. Phys Rev A 38:3098–3100
27. Lee C, Yang W, Parr RG (1988) Development of the Colle-Salvetti correlation-energy formula into a functional of the electron density. Phys Rev B 37:785–789
28. Powell RE (1968) Relativistic quantum chemistry. J Chem Educ 45:558–563
29. Pitzer K (1979) Relativistic effects on chemical properties. Acc Chem Res 12:271–276
30. Pyykko P, Desclaux JP (1979) Relativity and the periodic system of elements. Acc Chem Res 12:276–281
31. Pyykko P (1988) Relativistic effects in structural chemistry. Chem Rev 88:563–594
32. Liu W (2010) Ideas of relativistic quantum chemistry. Mol Phys 108:1679–1706
33. Fletcher R (1980) Practical methods of optimization, vol 1. Wiley, New York
34. te Velde G, Bickelhaupt FM, Baerends EJ, Guerra CF, van Gisbergen SJA (2001) Chemistry with ADF. J Comput Chem 22:931–967
35. Halgren TA, Lipscomb WN (1997) Chem Phys Lett 49:225–232
36. Guerra CF, Snijders JG, te Velde G, Baerends EJ (1998) Towards an order-N DFT method. Theor Chem Acc: Theory, Comput, Model (Theoretica Chimica Acta) 99:391–403
37. Zhang JF, Hao C, Li SM, Mi WH, Jin P (2007) Which configuration is more stable for La2@C_{80}, D_{3d} or D_{2h}? recomputation with ZORA methods within ADF. J Phys Chem C 111:7862–7867

38. van Lenthe E, Baerends EJ, Snijders JG (1993) Relativistic regular two-component Hamiltonians. J Chem Phys 99:4597–4610

39. van Lenthe E, Baerends EJ, Snijders JG (1994) Relativistic total energy using regular approximations. J Chem Phys 101:9783–9792

40. van Lenthe E, Ehlers AE, Baerends EJ (1999) Geometry optimizations in the zero order regular approximation for relativistic effects. J Chem Phys 110:8943–8953

41. Sun G, Kertesz M (2000) Theoretical ^{13}C NMR spectra of IPR isomers of fullerenes C_{60}, C_{70}, C_{72}, C_{74}, C_{76}, and C_{78} studied by density functional theory. J Phys Chem A104:7398–7403

42. Avent AG, Dubois D, Penicaud A, Taylor R (1997) The minor isomers and IR spectrum of [84]fullerene. J Chem Soc Perkin Trans 2:1907–1910

43. Rappoport D, Furche F (2009) Structure of endohedral fullerene Eu@C_{74}. Phys Chem Chem Phys 11:6353–6358